Cognitive Beamforming in Underlay Two-Way Relay Networks with Multi-Antenna Terminals

Yun CAO and Chintha Tellambura, *Fellow, IEEE*

***Abstract*—This paper studies an underlay cognitive network consisting of a two-way amplify-and-forward (AF) relay and two multi-antenna terminals (SU_1 and SU_2). Despite enhanced spectral efficiency and spectrum utilization, the underlay network is limited by low power transmissions and short coverage owing to secondary-to-primary (S2P) and primary-to-secondary (P2S) interference. To alleviate these, we consider beamforming at SU_1 and SU_2. However, concurrent bidirectional transmissions with the two-way relay complicates beamforming and power allocation. Nevertheless, we use the performance criterion of maximizing the worse received signal-to-interference-and-noise ratio (SINR) at SU_1 and SU_2. The resulting maximization problem for the optimal beamforming vectors and power allocation is a non-convex quadratically constraint quadratic program (QCQP), which is NP-hard. Thus we develop an iterative bisection search, but determining its feasibility at each iteration is still a non-convex NP-hard QCQP. We thus generate two equivalent interference minimization problems, which we solve by semidefinite relaxation (SDR). Simulation results show that our proposed optimal design improves SINR by as much as $20\,\mathrm{dB}$. We also propose sub-optimal maximal-ratio-transmission (MRT) and zero-forcing beamforming and maximal-ratio-transmission (ZFB-MRT), and develop their optimal power allocations. Importantly, the performance loss due to these sub-optimal strategies is modest (e.g. as low as $1\,\mathrm{dB}$ for ZFB-MRT with optimal power allocation).**

***Index Terms*—amplify-and-forward relaying, cognitive radio, beamforming, maximal-ratio-transmission, zero-forcing-and-maximal-ratio-transmission, power allocation, SINR balancing, two-way relay, underlay**

I. Introduction

The global mobile data traffic has been dramatically increasing since 2013 [1], which is expected to continue. For instance, a 10-fold increase over the 2013 traffic level is expected by 2018 [2]. Thus, the limited wireless spectrum is a critical bottleneck. Cognitive radio helps to address this problem by promoting the efficient use of spectrum. For instance, secondary users in underlay cognitive networks [3] are allowed to transmit provided the interference on the primary receivers (PRs) is below a predefined threshold (interference temperature limit) [4]. Therefore, such networks can reuse not only vacant radio bands, but also currently allocated radio bands. Thus, the underlay paradigm has the potential to mitigate both spectrum congestion and under-utilization. However, both primary-to-secondary (P2S) and secondary-to-primary (S2P) interference signals limit the achievable signal-to-interference-and-noise ratio (SINR). This means underlay nodes must

1) Reduce their transmit powers to comply with the S2P interference constraint,
2) Receive P2S interference, which in turn reduces the capacity of the secondary network.

In such a scenario, beamforming and relaying, used in the multiple-input multiple-output (MIMO) based 4G networks [5], [6] and also being investigated for the 5G wireless networks [7], [8], can be employed to improve the achievable SINR or data rate. Thus, underlay beamforming strategies have recently been studied extensively [9]–[32]. These studies consider both one-way and two-way relays.

For instance, [24]–[31] use amplify-and-forward (AF) relaying due to its advantages of low complexity and short delay [33]. Beamforming at the multiple antenna secondary base station and a one-way relay has been studied to maximize the data rate [24]. With perfect channel state information (CSI), distributed beamforming via multiple cooperative single-antenna AF relay nodes was investigated in [25]–[29]. Of these, [25]–[28] maximized the received SNR or minimized the interference at the primary receivers for one-way relays and [29] considered two-way relays. However, since full CSI may require too much overhead, [30] assumed the second-order channel statistics, and derived joint distributed beamforming and power allocation algorithms for two-way relays to maximize the worse SINR. A sub-optimal beamforming, maximal-ratio-transmission (MRT), for an underlay multi-antenna transmitter-receiver pair and a single-antenna relay node was studied [31], while the outage probability of zero-forcing beamforming and maximal-ratio-transmission (ZFB-MRT) for an underlay multi-antenna terminals and a single-antenna fixed-gain relay was analyzed in [32]. Except for [30] and [32], all these studies neglected the P2S interference.

In this paper, we consider an underlay network of a multi-antenna terminal pair (SU_1 and SU_2) and a single-antenna half-duplex two-way AF relay (R). In real applications, these two secondary terminals could be two wireless access points in two separate homes or two micro-cell base stations connected temporarily by the relay, which provides a wireless backhaul service. This system model is identical to the one in [31] except for the two-way relay. Thus, using the multiple access broadcast (MABC) two-way relaying protocol, two time slots are required for mutual information exchange between SU_1 and SU_2, which occurs as follows. In the first time slot, both

Yun CAO and Chintha Tellambura are with the Department of Electrical and Computer Engineering, University of Alberta, Edmonton, AB, Canada T6G 2V4 (Email: {cao7, chintha}@ece.ualberta.ca).

SU_1 and SU_2 transmit their data to R simultaneously. In the second time slot, R broadcasts an amplified version of the received signal. For this setup, we design cognitive beamforming vectors and power allocation jointly to reduce the overall outage probability, which is determined by the end-to-end outage probability of the weakest communication link [34]. Therefore, instead of minimizing the overall outage probability directly, cognitive beamforming and power allocation is used to maximize the worse of the two received SINRs at SU_1 and SU_2.

In previous work [30], we also investigated a network of multiple single-antenna relays and two single-antenna terminals. This current paper and [30] fundamentally differ in two ways. First, as mentioned above, both S2P and P2S interference signal limits the overall performance. However, both types of interference can not be mitigated in [30] due to the single-antenna constraint. In contrast, full interference mitigation is possible with multiple-antenna terminals in this paper as they provide enough spatial degrees of freedom. Second, [30] aims to reduce the burden of the CSI by using the relatively slowly-varying second-order channel statistics. Essentially, [30] deals with distributed beamforming for multiple relays and all single-antenna nodes.

To the best of our knowledge, beamforming design and power allocation for SU_1 and SU_2 considering both P2S and the S2P interference links have not been studied previously. We address this problem in two stages:

1) Receiving (Rx) beamforming,
2) Joint transmitting (Tx) beamforming and power allocation.

In stage 1), we convert Rx beamforming to the generalized Rayleigh-Ritz ratio maximization problem. However, in stage 2), joint Tx beamforming and power allocation is a quadratically constraint quadratic program (QCQP) with quadratic equality constraint, which is non-convex and NP-hard [35]. As the AF two-way relay requires two time slots for mutual data exchange, the selection of Tx beamforming vectors and power allocation in the first time slot affects the AF relay gain for the second time slot. The relay transmissions also must satisfy the interference constraint at the PR. Therefore, not only keeping the PR interference in both time slots below the interference limit, but also maximizing the minimum SINR of SU_1 and SU_2 over two time slots are required. Thus, these simultaneous requirements lead to a very difficult design problem. We find that the maximum achievable worse SINR can be found through a bi-section search along the parametric curve $\Phi(P_{1R}, P_{2R})$, where P_{jR} is the power received at the relay from SU_j ($j = 1, 2$). But, at each (P_{1R}, P_{2R}) pair, an $(M_1 + M_2)$-dimensional feasibility problem with regard to Tx beamforming and power allocation, where M_1 and M_2 are the numbers of antennas at the two terminals, respectively, needs to be solved. This feasibility problem is also a QCQP with quadratic equality constraint, which makes it non-convex and NP-hard [35]. We thus find two equivalent secondary-transmitter-to-primary-receiver interference minimization problems, and solve them using semidefinite relaxation (SDR). Although this bi-section search based process yields the optimal Tx beamforming vectors and power allocation, it has high complexity. We propose to reduce this complexity level by using two popular low-complexity beamforming schemes 1) MRT [31], [36]–[38], which maximizes the signal-to-noise ratio (SNR) [39], [40], and 2) ZFB-MRT [41], [42], which nullifies the interference while maximizing the desired signal power. These two methods have simple, closed-form solutions for TX beamforing vectors and thus eliminate the high computational complexity. However, the resulting beamforming vector is not optimal. Therefore, we will optimize the power allocation in order to partially recover the performance losses. In summary, the main contributions of our work are as follows:

1) We derive the optimal Rx beamforming vectors and prove that they are computed only from the CSIs, and is independently from the transmit powers and the Tx beamforming vectors.
2) We develop a joint optimal Tx beamforming and power allocation (JTBPA) algorithm, which solves non-convex, NP-hard optimization problem. Thus, JTBPA is based on the bi-section search along the received power pair (P_{1R}, P_{2R}). At each step, this leads to an $(M_1 + M_2)$-dimensional nonconvex feasibility determination of transmit powers and Tx beamforming vectors. We convert the feasibility problem into two interference minimization problems of M_1 and M_2 dimensions, which can be solved by SDR with running time of $\mathcal{O}(M_j^{4.5})$ ($j = 1, 2$). Since joint Tx beamforming and power allocation for underlay cognitive two-way relay network with multi-antenna terminals has not been investigated before, the proposed JTBPA algorithm provides a benchmark to evaluate other Tx beamforming and power allocation strategies.
3) Optimal power allocation is also developed for two low-complexity, sub-optimal beamforming schemes, MRT and ZFB-MRT.
4) An assessment of the relative merits of our proposed algorithms (JTBPA and sub-optimal Tx beamforming with optimal power allocation) is provided through extensive simulation and numerical results. For example, JTBPA increases the achievable SINR by as much as 20 dB compared with no Tx beamforming and equal power allocation (EPA). ZFB-MRT and MRT with optimal power allocation have 1 dB and 5 dB gaps from JTBPA, respectively. Moreover, ZFB-MRT performs satisfactorily even without power allocation. For instance, only 1 dB performance gap is incurred due to simply using the maximum power level.

The remainder of this paper is organized as follows. Section II describes the system model and formulates the optimization problem. The optimal relay gain and Rx beamforming vector are derived in Section III. The optimal JTBPA algorithm is developed in Section IV-A. The optimal power

allocation with MRT and ZFB-MRT is treated in Section IV-B. Numerical results comparing different Tx beamforming and power allocation methods are provided in Section V. Section VI concludes the paper.

Notations: Italics, bold lower-case italics and bold upper-case italics indicate scalars, vectors and matrices, respectively. $(\bullet)^*$, $(\bullet)^T$, $(\bullet)^{-1}$and $(\bullet)^H$ represent complex matrix conjugation, transpose, inverse, and Hermitian transpose, respectively. $\| \bullet \|$ is the L^2-norm. $\lambda(\boldsymbol{A}, \boldsymbol{B})$ is the generalized eigenvalue of matrices $\boldsymbol{A}$ and $\boldsymbol{B}$. $\mathcal{CN}(\mu, \sigma^2)$ denotes the circularly symmetric complex normal distribution with mean μ and variance σ^2. $\boldsymbol{I}_M$ is the $M \times M$ identity matrix. $\mathbb{C}$ is set of complex numbers.

II. System Configuration and Problem Formulation

A. System Model and Assumptions

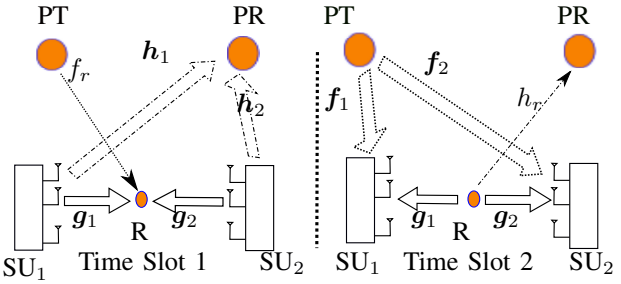

Fig. 1. Underlay Two-Way Relay Network with Multi-Antenna Terminals

The main assumptions of the system (Fig. 1) are as follows.

1) We consider a simple primary network of one single-antenna transmitter-receiver pair (PT-PR), Fig. 1. Note that multiple-antenna primary nodes will give rise to matrix interference channels and beamforming matrices. The resulting optimization problem is a generalization of this paper and may be investigated in future work.
2) The two underlay terminals SU$_1$ and SU$_2$ mutually exchange information via a half-duplex single-antenna AF two-way relay R, which requires two time slots. Our study is limited to a single-antenna relay for the following reasons. First, multiple antennas in some relays may be difficult due to the size and the cost constraints [33], [43]. Second, since such a multi-antenna relay allows beamforming at the relay, our work serves as a starting point. Third, beamforming design for the two terminals and a multiple-antenna relay can be a future work. The use of the half-duplex relay can mitigate the self-interference in full-duplex relays, which occurs at the receiving end because of the transmission from themselves [44].
3) SU$_j$ is equipped with $M_j \geq 2$ antennas and has the peak-power constraint P_j^{max} $(j = 1, 2)$.
4) We assume flat-fading wireless channels with the channels gains independent and identically distributed as $\mathcal{CN}(0, 1)$. The channel between SU$_j$ $(j = 1, 2)$ and the relay R is reciprocal. This reciprocity assumption is widely adopted in time-division-duplex (TDD) relaying systems [45], such as two-way relays.
5) We adopt the same assumption as in [22], [23], [25]–[28], [46] that the instantaneous CSI of all channels is perfectly known at every node. In practice, any node $x \in$\{SU$_1$, SU$_2$, R, PR\} can obtain the CSI of the y$\rightarrow$x ($y \in$\{SU$_1$, SU$_2$, R, PT\}) channel through pilot based channel estimation schemes [47]–[50], given that link exists (shown in Fig. 1). Then the obtained CSI is fed back to other nodes in Fig. 1 directly from x or indirectly from a band manager, who helps to exchange the CSI between nodes in the system [23], [46].
6) Since both secondary terminals know the CSI of all channels perfectly, each terminal SU$_j$ $(j = 1, 2)$ can calculate its own transmit power P_j, Tx beamforming vector $\boldsymbol{m}_j$, Rx beamforming vector $\boldsymbol{d}_j$, and the relay gain G by using the methods proposed in Section III and Section IV. Then, either SU$_1$ or SU$_2$ transmits the relay gain G to the relay.
7) The noise received at each node is additive white Gaussian noise (AWGN) of zero mean and σ^2 variance.
8) As in [31], [51], [52], perfect time synchronization is assumed between the primary and secondary networks. This will lead to the maximum interference power scenario.

B. Signal Models

When using the two-slot two-way relay (Fig. 1), the signal $\sqrt{P_j}\boldsymbol{m}_j s_j$ is transmitted from SU$_j$ $(j = 1, 2)$ to the relay R in the first time slot through the reciprocal channels $\boldsymbol{g}_j \in \mathbb{C}^{M_j \times 1}$, where P_j is the transmit power, s_j is the symbol to be transmitted, and $\boldsymbol{m}_j \in \mathbb{C}^{M_j \times 1}$ is the normalized Tx beamforming vector, $\|\boldsymbol{m}_j\|^2 = 1$. Simultaneously, PT transmits $x^{(1)}$ to PR with transmit power P_P. Therefore, the signal y_r and the interference $x_{int}^{(1)}$ received at the relay R and PR are given as

$$y_r = \sqrt{P_1}\boldsymbol{g}_1^T\boldsymbol{m}_1 s_1 + \sqrt{P_2}\boldsymbol{g}_2^T\boldsymbol{m}_2 s_2 + \sqrt{P_p} f_r x^{(1)} + n_r, \quad (1)$$

$$x_{int}^{(1)} = \sqrt{P_1}\boldsymbol{h}_1^T\boldsymbol{m}_1 s_1 + \sqrt{P_2}\boldsymbol{h}_2^T\boldsymbol{m}_2 s_2, \quad (2)$$

where $\boldsymbol{h}_j \in \mathbb{C}^{M_j \times 1}$ $(j = 1, 2)$ is the interference channel vector from SU$_j$ to PR, f_r is the complex interference channel gain from PT to R, and n_r is the AWGN at the relay.

In the second time slot, the relay R multiplies its received signal y_r with a complex relay gain $G \in \mathbb{C}$ and transmits the resultant. Then the relay generates the interference signal on PR as,

$$x_{int}^{(2)} = h_r G y_r, \quad (3)$$

where h_r is the complex channel gain from the relay to PR. Also, in time slot 2, PT transmits $x^{(2)}$ to PR with transmit power P_P. Then, the signal vector $\boldsymbol{y}_j$ received at SU$_j$ $(j = 1, 2)$ is given as,

$$\begin{aligned} y_j = {} & \sqrt{P_j} G \boldsymbol{g}_j \boldsymbol{g}_j^T \boldsymbol{m}_j s_j + \sqrt{P_{\bar{j}}} G \boldsymbol{g}_j \boldsymbol{g}_{\bar{j}}^T \boldsymbol{m}_{\bar{j}} s_{\bar{j}} \\ & + \sqrt{P_p} G \boldsymbol{g}_j f_r x^{(1)} + G \boldsymbol{g}_j n_r + \sqrt{P_p} \boldsymbol{f}_j x^{(2)} + \boldsymbol{n}_j, \end{aligned} \quad (4)$$

where $\boldsymbol{f}_j \in \mathbb{C}^{M_j \times 1}$ is the interference channel vector from

PT to SU$_j$, $\boldsymbol{n}_j \in \mathbb{C}^{M_j \times 1}$ is the vector of AWGN at SU$_j$, and $\bar{j} = 1$, if $j = 2$, and vice versa.

Knowing the relay gain G, the channel $\boldsymbol{g}_j$, its own transmit power P_j, Tx beamforming vector $\boldsymbol{m}_j$, and transmitted symbol s_j perfectly, SU$_j$ ($j = 1, 2$) can eliminate the self-interference part $\sqrt{P_j} G \boldsymbol{g}_j \boldsymbol{g}_j^T \boldsymbol{m}_j s_j$ before applying the Rx beamforming. After the self-interference cancellation and the Rx beamforming, the resulting signal $\hat{y}_j$ is represented as

$$\begin{aligned} \hat{y}_j = & \underbrace{\sqrt{P_{\bar{j}}} G \boldsymbol{d}_j^T \boldsymbol{g}_j \boldsymbol{g}_{\bar{j}}^T \boldsymbol{m}_{\bar{j}} s_{\bar{j}}}_{\text{Signal}} \\ & + \underbrace{\sqrt{P_p} G \boldsymbol{d}_j^T \boldsymbol{g}_j f_r x^{(1)} + \sqrt{P_p} \boldsymbol{d}_j^T \boldsymbol{f}_j x^{(2)}}_{\text{Interference}} \\ & + \underbrace{G \boldsymbol{d}_j^T \boldsymbol{g}_j n_r + \boldsymbol{d}_j^T \boldsymbol{n}_j}_{\text{Noise}}, \end{aligned} \tag{5}$$

where $\boldsymbol{d}_j \in \mathbb{C}^{M_j \times 1}$ ($j = 1, 2$) is the Rx beamforming vector satisfying $\|\boldsymbol{d}_j\|^2 = 1$.

Therefore, the instantaneous SINR at SU$_j$ ($j = 1, 2$) is calculated from (5) as

$$\text{SINR}_j = \frac{P_{\bar{j}} |G|^2 \boldsymbol{d}_j^H \boldsymbol{G}_j \boldsymbol{d}_j \boldsymbol{m}_{\bar{j}}^H \boldsymbol{G}_{\bar{j}} \boldsymbol{m}_{\bar{j}}}{\boldsymbol{d}_j^H (G^2 \Delta \boldsymbol{G}_j + \boldsymbol{F}_j) \boldsymbol{d}_j}, \tag{6}$$

where $\boldsymbol{G}_j = \boldsymbol{g}_j^* \boldsymbol{g}_j^T$, $\Delta = P_p |f_r|^2 + \sigma^2$, and $\boldsymbol{F}_j = P_p \boldsymbol{f}_j^* \boldsymbol{f}_j^T + \sigma^2 \boldsymbol{I}_{M_j}$. The interference powers at PR in time slot 1 and 2 are calculated from (2) and (3) as

$$P_I^{(1)} = P_1 \boldsymbol{m}_1^H \boldsymbol{H}_1 \boldsymbol{m}_1 + P_2 \boldsymbol{m}_2^H \boldsymbol{H}_2 \boldsymbol{m}_2, \tag{7}$$

$$P_I^{(2)} = |h_r|^2 |G|^2 (P_1 \boldsymbol{m}_1^H \boldsymbol{G}_1 \boldsymbol{m}_1 + P_2 \boldsymbol{m}_2^H \boldsymbol{G}_2 \boldsymbol{m}_2 + \Delta), \tag{8}$$

where $\boldsymbol{H}_j = \boldsymbol{h}_j^* \boldsymbol{h}_j^T$ ($j = 1, 2$).

Note that, since only the signal power levels are considered, e.g. SINR (6) and interference power at PR (8), the phase $\angle(G)$ of G is irrelevant. For this reason, we set $\angle(G) = 0$ and model the relay gain G as a positive real-valued scale hereafter. Then, $|G|^2$ in (6) and (8) is replaced by G^2.

C. Beamforming Design Criteria

As mentioned in Section I, we aim at choosing the relay gain G, transmit powers P_j, Tx beamforming vectors $\boldsymbol{m}_j$ and Rx beamforming vectors $\boldsymbol{d}_j$ ($j = 1, 2$) to maximize $\min(\text{SINR}_1, \text{SINR}_2)$. Recall that, the interference at PR ($P_I^{(1)}$ and $P_I^{(2)}$) received at PR must be lower than the interference temperature limit (I_{th}). Meanwhile, the transmit powers P_j ($j = 1, 2$) can not exceed their maximum values P_j^{max}. Putting all these conditions together, the optimization problem is formulated as

$$\begin{aligned} \text{(P-1)} \quad \max_{P_j, G, \boldsymbol{m}_j, \boldsymbol{d}_j} \quad & \min\{\text{SINR}_1, \text{SINR}_2\} \\ \text{s.t.} \quad & \|\boldsymbol{m}_j\|^2 = 1, \ \|\boldsymbol{d}_j\|^2 = 1, && \text{(9a)} \\ & P_1 \le P_1^{max}, \ P_2 \le P_2^{max}, && \text{(9b)} \\ & P_I^{(1)} \le I_{th}, \ P_I^{(2)} \le I_{th}, && \text{(9c)} \\ & j = 1, 2. \end{aligned}$$

III. Optimal Relaying Gain and Receiving Beamforming

We first derive the optimal relay gain G and Rx beamforming vectors $\boldsymbol{d}_j$ ($j = 1, 2$) in this section. Since among the constraints (9a)-(9c), only $P_I^{(2)} \le I_{th}$ depends on the relay gain G, when the optimal value of (P-1) is achieved, $P_I^{(2)} = I_{th}$ must hold. Otherwise, if (P-1) achieves its optimal value SINR^o and $P_I^{(2)} < I_{th}$, G can be increased to $\hat{G}$ such that $P_I^{(2)} = I_{th}$. Then substituting $\hat{G}$ into (6) results in higher SINR$_j$ ($j = 1, 2$) and consequently a worse SINR, which is higher than SINR^o, is achieved, which contradicts that SINR^o is the optimal value. Therefore, G should be chosen as

$$G = \sqrt{\frac{I_{th}}{|h_r|^2 (P_1 \boldsymbol{m}_1^H \boldsymbol{G}_1 \boldsymbol{m}_1 + P_2 \boldsymbol{m}_2^H \boldsymbol{G}_2 \boldsymbol{m}_2 + \Delta)}}. \tag{10}$$

Substituting (10) into (6), SINR$_j$ ($j = 1, 2$) can be reformulated as

$$\text{SINR}_j = \frac{P_{\bar{j}R} \gamma_{Rj}}{P_{1R} + P_{2R} + (\gamma_{Rj} + 1)\Delta}, \tag{11}$$

where $P_{jR} = P_j \boldsymbol{m}_j^H \boldsymbol{G}_j \boldsymbol{m}_j$, and $\gamma_{Rj} = \frac{I_{th} \boldsymbol{d}_j^H \boldsymbol{G}_j \boldsymbol{d}_j}{|h_r|^2 \boldsymbol{d}_j^H \boldsymbol{F}_j \boldsymbol{d}_j}$ ($j = 1, 2$). Note that P_{jR} and γ_{Rj} ($j = 1, 2$) are the signal powers from SU$_j$ to R and the SINR from R to SU$_j$, respectively.

Lemma 1. *SINR$_j$ in* (11) *increases with the increase in* γ_{Rj}.

Proof. Since SINR$_j > 0$ and $\gamma_{Rj} > 0$, we have

$$\begin{aligned} \frac{\partial \text{SINR}_j}{\partial \gamma_{Rj}} &= \frac{\gamma_{\bar{j}R}[\gamma_{1R} + \gamma_{2R} + (\gamma_{Rj} + 1)\Delta] - \Delta \gamma_{\bar{j}R} \gamma_{Rj}}{[\gamma_{1R} + \gamma_{2R} + (\gamma_{Rj} + 1)\Delta]^2} \\ &= \frac{\gamma_{\bar{j}R}[\gamma_{1R} + \gamma_{2R} + \Delta]}{[\gamma_{1R} + \gamma_{2R} + (\gamma_{Rj} + 1)\Delta]^2} > 0. \end{aligned}$$

Thus, SINR$_j$ increases with γ_{Rj}. □

By applying Lemma 1, we obtain the following lemma.

Lemma 2. *Let $\hat{\boldsymbol{d}}_j$ ($j = 1, 2$) be the vector such that γ_{Rj} achieves its maximum value γ_{Rj}^{max}. Then, $\hat{\boldsymbol{d}}_j$ ($j = 1, 2$) is an optimal solution of (P-1) .*

Proof. Since γ_{Rj} ($j = 1, 2$) achieves its maximum value γ_{Rj}^{max} when $\boldsymbol{d}_j = \hat{\boldsymbol{d}}_j$, to prove Lemma 2 is equivalent to prove that γ_{Rj}^{max} ($j = 1, 2$) is an optimal solution of (P-1). Then, we assume that when (P-1) achieves its optimal value SINR^o=$\min$(SINR$_1$, SINR$_2$), at least one of $\gamma_{R1} < \gamma_{R1}^{max}$ and $\gamma_{R2} < \gamma_{R2}^{max}$ holds. This leads to two cases:

1) When SINR^o is achieved, only one of $\gamma_{Rj} < \gamma_{Rj}^{max}$ ($j = 1, 2$) holds.
   Without loss of generality, we assume that $\gamma_{R1} < \gamma_{R1}^{max}$ and $\gamma_{R2} = \gamma_{R2}^{max}$. If γ_{R1} is increased to γ_{R1}^{max}, by applying Lemma 1, SINR$_1$ will increase as well. Then, there are two cases to consider: a) SINR^o =SINR$_2$ ≤SINR$_1$, and b) SINR^o =SINR$_1$ <SINR$_2$. In Case a), increasing SINR$_1$ will achieve the same SINR^o. Therefore, γ_{R1}^{max} is also an optimal solution of (P-1) in this case. In Case b), increasing SINR$_1$ will result in an SINR higher than

SINR^o. This contradicts that SINR^o is the optimal value of (P-1).

2) When SINR^o is achieved, both of $\gamma_{Rj} < \gamma_{Rj}^{max}$ ($j = 1, 2$) hold.
In this case, if both of γ_{Rj} ($j = 1, 2$) are increased to their maximum value γ_{Rj}^{max}, by applying Lemma 1, SINR_j will increase as well. Then, an $\min(\text{SINR}_1, \text{SINR}_2) > \text{SINR}^o$ is achieved. This contradicts that SINR^o is the optimal value of (P-1).

Therefore, considering both Case 1) and 2), γ_{Rj}^{max} ($j = 1, 2$) is an optimal solution of (P-1). □

Then, according to Lemma 2, $\boldsymbol{d}_j$ ($j = 1, 2$) should be chosen to maximize γ_{Rj}. It is known that the generalized Rayleigh-Ritz ratio in the form as $\frac{\boldsymbol{d}_j^H \boldsymbol{G}_j \boldsymbol{d}_j}{\boldsymbol{d}_j^H \boldsymbol{F}_j \boldsymbol{d}_j}$ is maximized when $\boldsymbol{d}_j$ is chosen as (12) by exploiting the definition of $\boldsymbol{G}_j$ [53] and its maximum value γ_{Rj}^{max} is computed as (13) by using the Sherman-Morrison formula [54]:

$$\boldsymbol{d}_j = \frac{(P_p \boldsymbol{f}_j^* \boldsymbol{f}_j^T + \sigma^2 I_{M_j})^{-1} \boldsymbol{g}_j^*}{|(P_p \boldsymbol{f}_j^* \boldsymbol{f}_j^T + \sigma^2 I_{M_j})^{-1} \boldsymbol{g}_j^*|}. \tag{12}$$

$$\gamma_{Rj}^{max} = \frac{I_{th}}{|h_r|^2}(\|\boldsymbol{g}_j\|^2 - \frac{P_p |\boldsymbol{f}_j^T \boldsymbol{g}_j^*|^2}{\sigma^2(\sigma^2 + P_p \|\boldsymbol{f}_j\|^2)}) \tag{13}$$

Note that the Rx beamforming vectors ($\boldsymbol{d}_j$, $j = 1, 2$) is calculated only from the CSIs. For simplicity, we denote γ_{Rj}^{max} as γ_j ($j = 1, 2$) hereafter and reformulate (P-1) into (P-2), which is an optimization problem with regard to the transmit powers P_j and Tx beamforming vector $\boldsymbol{m}_j$ ($j = 1, 2$). However, (P-2) is a non-convex optimization problem.

IV. Transmitting Beamforming and Power Allocation

In this section, we develop the optimal JTBPA algorithm for (P-2) for Tx beamforming vectors $\boldsymbol{m}_j$ and powers P_j ($j = 1, 2$). To reduce the high computational complexity, we also propose low-complexity, sub-optimal beamformers ZFB-MRT and MRT. In this case, $\boldsymbol{m}_j$ have closed-form solutions and we optimize P_j ($j = 1, 2$) to mitigate the performance loss due to the suboptimal $\boldsymbol{m}_j$ ($j = 1, 2$).

A. Optimal Joint Transmitter-Side Beamforming and Power Allocation

To find the optimal Tx beamforming vectors and power allocation, we observe the following lemma on the optimization problem (P-2).

Lemma 3. *There exists an optimal solution $(P_1^o, P_2^o, \boldsymbol{m}_1^o, \boldsymbol{m}_2^o)$ to (P-2) such that the corresponding optimal SINRs at the two terminals satisfying $\text{SINR}_1^o = \text{SINR}_2^o$.*

Proof. Let $(P_1^o, P_2^o, \boldsymbol{m}_1^o, \boldsymbol{m}_2^o)$ be an optimal solution to (P-2). We assume that $\text{SINR}_1^o < \text{SINR}_2^o$. Therefore the corresponding optimal value SINR^o of (P-2) satisfies $\text{SINR}^o = \text{SINR}_1^o$.

Define $\kappa = \frac{\text{SINR}_1^o}{\text{SINR}_2^o}$, then $\kappa < 1$ and $\text{SINR}^o = \kappa \text{SINR}_2^o$. Define a new power allocation $\tilde{P}_1 = \kappa P_1^o$, $\tilde{P}_2 = P_2^o$. $(P_1^o, P_2^o, \boldsymbol{m}_1^{opt}, \boldsymbol{m}_2^{opt})$ is also a feasible point of (P-2), and the resulting $\widetilde{\text{SINR}_1} > \text{SINR}_1^o$ and $\widetilde{\text{SINR}_2} > \text{SINR}^o$. This contradicts that $(P_1^o, P_2^o, \boldsymbol{m}_1^o, \boldsymbol{m}_2^o)$ is an optimal solution to (P-2). □

By applying Lemma 3, (P-2) is reformulated as

$$\begin{aligned}
\text{(P-3)} \quad \max_{P_1, P_2, \boldsymbol{m}_1, \boldsymbol{m}_2} \quad & \frac{\gamma_1 P_{2R} - \gamma_2 P_{1R}}{(\gamma_1 - \gamma_2)\Delta} \\
\text{s.t.} \quad & \|\boldsymbol{m}_j\|^2 = 1,\ j = 1, 2, && \text{(15a)} \\
& P_1 \le P_1^{max},\ P_2 \le P_2^{max}, && \text{(15b)} \\
& P_1 \boldsymbol{m}_1^H \boldsymbol{H}_1 \boldsymbol{m}_1 + P_2 \boldsymbol{m}_2^H \boldsymbol{H}_2 \boldsymbol{m}_2 \le I_{th} && \text{(15c)} \\
& \Phi(P_{1R}, P_{2R}) = 0, && \text{(15d)}
\end{aligned}$$

where

$$\begin{aligned}
\Phi(P_{1R}, P_{2R}) = {} & \gamma_1 P_{2R}^2 - \gamma_2 P_{1R}^2 + (\gamma_1 - \gamma_2) P_{1R} P_{2R} \\
& + \gamma_1(\gamma_2 + 1)\Delta P_{2R} - \gamma_2(\gamma_1 + 1)\Delta P_{1R}.
\end{aligned} \tag{16}$$

(P-3) is a QCQP with quadratic equality constraint, which is non-convex and NP-hard [35]. Note that (15d) is a hyperbolic curve passing the origin point $(P_{1R}, P_{2R}) = (0, 0)$. To solve (P-3), three cases need to be considered: (1) $\gamma_1 > \gamma_2$, (2) $\gamma_1 = \gamma_2$ and (3) $\gamma_1 < \gamma_2$. Since $\gamma_1 = \gamma_2$ is a zero-probability event, we neglect this case here. If $\gamma_1 > \gamma_2$, $(P_1, P_2, \boldsymbol{m}_1, \boldsymbol{m}_2)$ should be chosen such that $\gamma_1 P_{2R} - \gamma_2 P_{1R}$ is positive. Meanwhile, it is easy to prove that the hyperbolic curve $\Phi(P_{1R}, P_{2R}) = 0$ always satisfies this requirement when $P_{jR} > 0$ ($j = 1, 2$). Similarly, the hyperbolic curve $\Phi(P_{1R}, P_{2R}) = 0$ always satisfies $\gamma_1 P_{2R} - \gamma_2 P_{1R} < 0$ in the first phase when $\gamma_1 < \gamma_2$. Therefore, there must exist a solution $(P_1, P_2, \boldsymbol{m}_1, \boldsymbol{m}_2)$ such that $\Phi(P_{1R}, P_{2R}) = 0$ and the optimal value of (P-3) is achieved.

Accordingly, a bi-section search along the hyperbolic curve $\Phi(P_{1R}, P_{2R}) = 0$ can be applied to find the optimal (P_{1R}, P_{2R}) until the stopping threshold η is satisfied (Step 4 in JTBPA). With fixed $\text{SINR}_1 = \text{SINR}_2 = t_{\text{mid}}$, $(P_{1R_{\text{mid}}}, P_{2R_{\text{mid}}})$ is obtained by solving the equations $\frac{\gamma_1 P_{2R_{\text{mid}}} - \gamma_2 P_{1R_{\text{mid}}}}{(\gamma_1 - \gamma_2)\Delta} = t_{\text{mid}}$ and (15d). Then, the problem (P-3) is reduced to a feasibility problem

$$\begin{aligned}
\text{(P-4)} \quad \text{find} \quad & \hat{\boldsymbol{m}}_1, \hat{\boldsymbol{m}}_2 \\
\text{s.t.} \quad & \|\hat{\boldsymbol{m}}_j\|^2 \le P_j^{max},\ j = 1, 2, && \text{(17a)} \\
& \hat{\boldsymbol{m}}_1^H \boldsymbol{H}_1 \hat{\boldsymbol{m}}_1 + \hat{\boldsymbol{m}}_2^H \boldsymbol{H}_2 \hat{\boldsymbol{m}}_2 \le I_{th}, && \text{(17b)} \\
& \hat{\boldsymbol{m}}_j^H \boldsymbol{G}_j \hat{\boldsymbol{m}}_j = \gamma_{jR_{\text{mid}}},\ j = 1, 2, && \text{(17c)}
\end{aligned}$$

where $\hat{\boldsymbol{m}}_j = \sqrt{P_j}\boldsymbol{m}_j$ ($j = 1, 2$).

Note that (P-4) is an $(M_1 + M_2)$-dimensional nonconvex feasibility problem with both quadratic inequality and equality constraints, which is NP-hard [35]. To reduce its dimension, we transfer it into two M_j-dimensional ($j = 1, 2$) interference minimization problems (P-5).

$$\begin{aligned}
\text{(P-5)} \quad \min_{\hat{\boldsymbol{m}}_j} \quad & \hat{\boldsymbol{m}}_j^H \boldsymbol{H}_j \hat{\boldsymbol{m}}_j \\
\text{s.t.} \quad & \|\hat{\boldsymbol{m}}_j\|^2 \le P_j^{max}, && \text{(18a)} \\
& \hat{\boldsymbol{m}}_j^H \boldsymbol{G}_j \hat{\boldsymbol{m}}_j = \gamma_{jR_{\text{mid}}}, && \text{(18b)} \\
& j = 1, 2,
\end{aligned}$$

$$\text{(P-2)} \quad \max_{P_1,\, P_2,\, \boldsymbol{m}_1,\, \boldsymbol{m}_2} \quad \min\{\frac{\gamma_1 P_{2R}}{P_{1R}+P_{2R}+(\gamma_1+1)\Delta}, \frac{\gamma_2 P_{1R}}{P_{1R}+P_{2R}+(\gamma_2+1)\Delta}\}$$

$$\text{s.t.} \quad \|\boldsymbol{m}_j\|^2 = 1,\, j=1,\, 2, \tag{14a}$$

$$P_1 \le P_1^{max},\, P_2 \le P_2^{max}, \tag{14b}$$

$$P_1 \boldsymbol{m}_1^H \boldsymbol{H}_1 \boldsymbol{m}_1 + P_2 \boldsymbol{m}_2^H \boldsymbol{H}_2 \boldsymbol{m}_2 \le I_{th}. \tag{14c}$$

where $\hat{\boldsymbol{m}}_j^H \boldsymbol{H}_j \hat{\boldsymbol{m}}_j$ is the SU$_j$ $\rightarrow$PR interference power in the first time slot. If we define $\boldsymbol{X}_j = \hat{\boldsymbol{m}}_j \hat{\boldsymbol{m}}_j^H$, (P-5) is equivalent to

$$\text{(P-6)} \quad \min_{\hat{\boldsymbol{m}}_j} \quad \text{Tr}(\boldsymbol{H}_j \boldsymbol{X}_j)$$

$$\text{s.t.} \quad \text{Tr}(\boldsymbol{X}_j) \le P_j^{max}, \tag{19a}$$

$$\text{Tr}(\boldsymbol{G}_j \boldsymbol{X}_j) = \gamma_{jR_{\text{mid}}}, \tag{19b}$$

$$\boldsymbol{X} \succeq \boldsymbol{0},\, \text{rank}\{\boldsymbol{X}\} = 1. \tag{19c}$$

which can be solved by SDR technique [35]. In SDR, the rank-1 constraint (19c) is dropped and the optimal solution $\boldsymbol{X}_j^\star$ to the resultant problem is solved via interior-point algorithms [55]. If the solution satisfies rank-1 constraint, then it will be optimal to (P-6) and $\hat{\boldsymbol{m}}_j$ can be extracted from $\boldsymbol{X}_j^\star$. Note that, it has been shown in [35], [56] that with only two constraints, the SDR of (P-6) always has a rank-1 solution, rank$\{\boldsymbol{X}_j^\star\} = 1$, whenever the optimization problem is feasible. Once the optimal $\hat{\boldsymbol{m}}_j^H \boldsymbol{H}_j \hat{\boldsymbol{m}}_j$ of (P-5) is found with $j = 1$ and 2, we compare the sum of them with the interference threshold I_{th}. If $\hat{\boldsymbol{m}}_1^H \boldsymbol{H}_1 \hat{\boldsymbol{m}}_1 + \hat{\boldsymbol{m}}_2^H \boldsymbol{H}_2 \hat{\boldsymbol{m}}_2 \le I_{th}$, it is equivalent to that (P-4) is feasible, otherwise (P-4) is not feasible.

The analysis above is concluded in the JTBPA algorithm, where the initial point t_{mid} of the bi-section search is determined by the lower bound and the upper bound of the achievable SINR. The lower bound t_{low} is simply chosen as zero, while the upper bound t_{up} is chosen as the optimal value of (P-7), which drops the constraint (15c) in (P-3) and maximizes the objective function with regard to P_{jR} ($j = 1,\, 2$). The first two constraints in (P-7) result from the fact that the maximum value of $P_{jR} = P_j \boldsymbol{m}_j^H \boldsymbol{G}_j \boldsymbol{m}_j$ ($j = 1,\, 2$) equals to the multiplication of P_j^{max} and the principle eigenvalue of $\boldsymbol{G}_j$, which is Tr$(\boldsymbol{G}_j)$ according to the definition of $\boldsymbol{G}_j$. Note that the optimal value of (P-7) is achieved when $(P_{1R},\, P_{2R})$ is as far from the line $P_{2R} = \frac{\gamma_2}{\gamma_1} P_{1R}$ as possible for both $\gamma_1 < \gamma_2$ and $\gamma_1 > \gamma_2$. Meanwhile, $(P_{1R},\, P_{2R})$ must be on the hyperbolic curve $\Phi(P_{1R},\, P_{2R}) = 0$. Since when $P_{1R} \ge 0$, $P_{2R} \ge 0$, $\Phi(P_{1R}, P_{2R}) = 0$ monotonically increases and has only one crosspoint with $P_{2R} = \frac{\gamma_2}{\gamma_1} P_{1R}$ at $(0,\, 0)$, the distance from points $(P_{1R},\, P_{2R})$ on the hyperbolic curve to the line $P_{2R} = \frac{\gamma_2}{\gamma_1} P_{1R}$ increases with the increase in P_{1R}. Otherwise, $\Phi(P_{1R}, P_{2R}) = 0$ and $P_{2R} = \frac{\gamma_2}{\gamma_1} P_{1R}$ would have another crosspoint when $P_{1R} > 0$, $P_{2R} > 0$. Therefore, let $(P_1^{max}\text{Tr}(\boldsymbol{G}_1),\, P_{2R}^{(1)})$ and $(P_{1R}^{(2)},\, P_2^{max}\text{Tr}(\boldsymbol{G}_2))$ be the crosspoints of $P_{1R} = P_1^{max}\text{Tr}(\boldsymbol{G}_1)$ and $P_{2R} = P_2^{max}\text{Tr}(\boldsymbol{G}_2)$ with $\Phi(P_{1R}, P_{2R}) = 0$, respectively, then the one satisfying both (20a) and (20b) must be the optimal solution to (P-7).

$$\text{(P-7)} \quad \max_{P_{1R},\, P_{2R}} \quad \frac{\gamma_1 P_{2R} - \gamma_2 P_{1R}}{(\gamma_1 - \gamma_2)\Delta}$$

$$\text{s.t.} \quad P_{1R} \le P_1^{max}\text{Tr}(\boldsymbol{G}_1), \tag{20a}$$

$$P_{2R} \le P_2^{max}\text{Tr}(\boldsymbol{G}_2), \tag{20b}$$

$$\Phi(P_{1R}, P_{2R}) = 0 \tag{20c}$$

Algorithm JTBPA: Optimal Joint Beamforming and Power Allocation

Input : $\boldsymbol{G}_1$, $\boldsymbol{G}_2$, $\boldsymbol{H}_1$, $\boldsymbol{H}_2$, $\boldsymbol{F}_1$, $\boldsymbol{F}_2$, Δ, h_r, I_{th}, P_1^{max}, P_2^{max}

Output: SINR, P_1, P_2, $\boldsymbol{m}_1$, $\boldsymbol{m}_2$, $\boldsymbol{d}_1$, $\boldsymbol{d}_2$, G

Compute γ_j and $\boldsymbol{d}_j$, $(j = 1, 2)$ using (13) and (12), respectively;

Compute $(P_1^{max}\text{Tr}(\boldsymbol{G}_1),\, P_{2R}^{(1)})$ and $(P_{1R}^{(2)},\, P_2^{max}\text{Tr}(\boldsymbol{G}_2))$ being the crosspoints of $P_{1R} = P_1^{max}\text{Tr}(\boldsymbol{G}_1)$ and $P_{2R} = P_2^{max}\text{Tr}(\boldsymbol{G}_2)$ with $\Phi(P_{1R}, P_{2R}) = 0$ respectively. Chose the one satisfying both (20a) and (20b) as the solution to (P-7), compute its optimal value and set the result to t_{up};

$t_{\text{low}} = 0$, $t_{\text{mid}} = \frac{t_{\text{up}} + t_{\text{low}}}{2}$, $t_{\text{mid}}^{\text{old}} = Inf$;

while $|t_{mid} - t_{mid}^{old}| > \eta$ **do**

  $t_{\text{mid}}^{\text{old}} = t_{\text{mid}}$;

  Calculate $(P_{1R_{\text{mid}}},\, P_{2R_{\text{mid}}})$ such that both $\frac{\gamma_1 P_{2R_{\text{mid}}} - \gamma_2 P_{1R_{\text{mid}}}}{(\gamma_1 - \gamma_2)\Delta} = t_{\text{mid}}$ and (15d) are satisfied;

  Find $\hat{\boldsymbol{m}}_j^H \boldsymbol{H}_j \hat{\boldsymbol{m}}_j$ and $\hat{\boldsymbol{m}}_j$ by solving (P-5) using SDR $(j = 1,\, 2)$;

  if $\hat{\boldsymbol{m}}_1^H \boldsymbol{H}_1 \hat{\boldsymbol{m}}_1 + \hat{\boldsymbol{m}}_2^H \boldsymbol{H}_2 \hat{\boldsymbol{m}}_2 \le I_{th}$ **then**

    $t_{\text{low}} = t_{\text{mid}}$;

    $P_j = \|\hat{\boldsymbol{m}}_j\|^2$, $\boldsymbol{m}_j = \frac{1}{\sqrt{P_j}} \hat{\boldsymbol{m}}_j$, $(j = 1,\, 2)$;

  else $t_{\text{up}} = t_{\text{mid}}$;

  end

  $t_{\text{mid}} = \frac{t_{\text{up}} + t_{\text{low}}}{2}$;

end

$G = \sqrt{\frac{I_{th}}{|h_r|^2 (P_1 \boldsymbol{m}_1^H \boldsymbol{G}_1 \boldsymbol{m}_1 + P_2 \boldsymbol{m}_2^H \boldsymbol{G}_2 \boldsymbol{m}_2 + \Delta)}}$;

return SINR, P_1, P_2, $\boldsymbol{m}_1$, $\boldsymbol{m}_2$, $\boldsymbol{d}_1$, $\boldsymbol{d}_2$, G.

Although JTBPA optimally computes P_j and $\boldsymbol{m}_j$ $(j = 1,\, 2)$, the bi-section search and the use of SDR result in high computational complexity (see Section IV-C).

B. Optimal Power Allocation with Different Transmitter-Side Beamforming

Since JTBPA has relatively high computational complexity (see Table II), we derive sub-optimal Tx beamforming vectors based on two different widely-used, low-complexity Tx beamforming strategies (MRT and ZFB-MRT). Contingent upon their beamforming vectors, we will optimize the power allocation to partially compensate for the performance loss. Note that whilst such a two-stage solution is necessarily sub-optimal, significant complexity savings are possible.

1) MRT: The Tx beamforming vector $\boldsymbol{m}_j^{MRT}$ $(j = 1, 2)$ is chosen as

$$\boldsymbol{m}_j^{MRT} = \frac{\boldsymbol{g}_j^*}{\|\boldsymbol{g}_j\|} \tag{21}$$

to maximize the received signal power at the relay R.

2) ZFB-MRT: We first find the sub-space Ψ_j, which is orthogonal to the SU$_j$ →PR interference channels $\boldsymbol{h}_j$ $(j = 1, 2)$, then project $\boldsymbol{g}_j$ onto Ψ_j, which results in the beamforming vector

$$\boldsymbol{m}_j^{ZFB-MRT} = \frac{\Psi_j \boldsymbol{g}_j^*}{\sqrt{\boldsymbol{g}_j^T \Psi_j \boldsymbol{g}_j^*}}, \tag{22}$$

where $\Psi_j = I - \frac{\boldsymbol{h}_j^* \boldsymbol{h}_j^T}{\|\boldsymbol{h}_j\|^2}$. This projection eliminates the interference from SU$_j$'s transmission to PR. Therefore, constraint (23b) is always satisfied. In principle, this allows for an arbitrary increase in the transmit powers of the terminals.

3) Optimal Power Allocation (OPA): With both MRT and ZFB-MRT, the beamforming vectors $\boldsymbol{m}_j$ $(j = 1, 2)$ have closed-form expressions given by (21) and (22). Then the optimization problem (P-3) is reduced to the optimal power allocation problem,

$$\begin{aligned} \text{(P-8)} \quad \max_{P_1, P_2} \quad & \frac{P_2\gamma_1\tilde{P_{2R}} - P_1\gamma_2\tilde{P_{1R}}}{(\gamma_1 - \gamma_2)\Delta} \\ \text{s.t.} \quad & P_1 \le P_1^{max},\ P_2 \le P_2^{max}, && \text{(23a)} \\ & a_1P_1 + a_2P_2 \le I_{th}, && \text{(23b)} \\ & \Phi(P_1, P_2) = 0, && \text{(23c)} \end{aligned}$$

where $\tilde{P_{jR}} = \boldsymbol{m}_j^H \boldsymbol{G}_j \boldsymbol{m}_j$, $a_1 = \boldsymbol{m}_1^H \boldsymbol{H}_1 \boldsymbol{m}_1$, $a_2 = \boldsymbol{m}_2^H \boldsymbol{H}_2 \boldsymbol{m}_2$, and

$$\begin{aligned} \Phi(P_1, P_2) =& \gamma_1 \tilde{P_{2R}}^2 P_2^2 - \gamma_2 \tilde{P_{1R}}^2 P_1^2 + (\gamma_1 - \gamma_2)\tilde{P_{1R}}\tilde{P_{2R}} P_1 P_2 \\ & + \gamma_1(\gamma_2 + 1)\Delta \tilde{P_{2R}} P_2 - \gamma_2(\gamma_1 + 1)\Delta \tilde{P_{1R}} P_1. \end{aligned} \tag{24}$$

It is easy to prove that with the optimal power allocation (P_1, P_2), at least one of the three constraints (23a) and (23b) is satisfied with equality, because otherwise we can increase P_1 or P_2 to achieve a better solution. Consequently, the optimal power allocation (P_1, P_2) lies on the red solid line in Fig. 2, which is formed by (23a) and (23b). Therefore, the optimal power allocation (P_1, P_2) must be the cross point of the red solid line and the hyperbolic curve $\Phi(P_1, P_2) = 0$. This cross point can be found by first calculating the cross-points $(P_1^{(1)}, P_2^{(1)})$, $(P_1^{(2)}, P_2^{(2)})$ and $(P_1^{(3)}, P_2^{(3)})$of $\Phi(P_1, P_2) = 0$ with $P_1 = P_1^{max}$, $P_2 = P_2^{max}$, and $a_1P_1 + a_2P_2 = I_{th}$, respectively, according to (25a)–(25c), then choosing the one satisfying both (23a) and (23b).

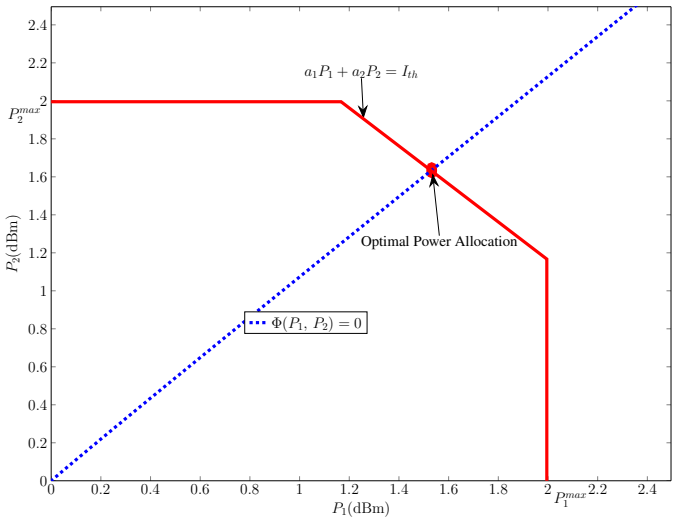

Fig. 2. Optimal Power Allocation

C. Complexity Analysis

Since JTBPA does a bi-section search and applies SDR at each search point, its running time can be estimated as follows. The worst-case total number of iterations in the bi-section search is given as $\log_2(\frac{t_{\text{up}} - t_{\text{low}}}{\eta})$ [57], where t_{up} and t_{low} are the upper and lower bounds of the bi-section search, respectively. At each search point, SDR requires running time of $\mathcal{O}(M_1^{4.5} + M_2^{4.5})$ [35] to solve two interference minimization problems. Therefore, the total running time of JTBPA is given as $\mathcal{O}(\log_2(\frac{t_{\text{up}} - t_{\text{low}}}{\eta})(M_1^{4.5} + M_2^{4.5}))$.

For both MRT and ZFB-MRT, only matrix multiplication is utilized which requires running time of $\mathcal{O}(M_j^2)$ to compute the Tx beamforming vectors $\boldsymbol{m}_j$ $(j = 1, 2)$. Then, the optimal power is obtained through numerical calculations, which requires constant time. Therefore, the complexity of MRT or ZFB-MRT with optimal power allocation is significantly lower than JTBPA. A clear comparison is shown in Table I

V. Numerical Results

Since our system (Fig. 1) has not previously been investigated in the literature, directly comparisons are unavailable. However, for this system, our simulation results compare five different beamforming and power allocation schemes: 1) JTBPA, 2) ZFB-MRT with optimal power allocation (ZFB-MRT-OPA), 3) ZFB-MRT with maximum power (ZFB-MRT-MP), 4) MRT with optimal power allocation (MRT-OPA), and 5) Equal power allocation (EPA). In the EPA scheme, $\boldsymbol{m}_j$ is set to $\frac{1}{\sqrt{M_j}}\mathbf{1}$ $(j = 1, 2)$, where the denominator is the normalizing factor, and P_j is set to P, where $P = \min(\frac{I_{th}}{|\boldsymbol{h}_1^T \boldsymbol{m}_1|^2 + |\boldsymbol{h}_2^T \boldsymbol{m}_2|^2}, P^{max})$. Schemes 1)-5) use the optimal Rx beamforming and relay gain (Section III). To analyze the SINR loss due to the underlay cognitive mode, we also show the results of the Ideal case. The Ideal case includes only

$$P_1^{(1)} = \frac{-\xi_1 - \sqrt{\xi_1^2 - 4\zeta_1\varrho_1}}{2\zeta_1},\ P_2^{(1)} = P_2^{max}, \tag{25a}$$

$$P_1^{(2)} = P_1^{max},\ P_2^{(2)} = \frac{-\xi_2 + \sqrt{\xi_2^2 - 4\zeta_2\varrho_2}}{2\zeta_2}, \tag{25b}$$

$$P_1^{(3)} = \frac{-\xi_3 - \sqrt{\xi_3^2 - 4\zeta_3\varrho_3}}{2\zeta_3},\ P_2^{(3)} = \frac{I_{th}}{a_1} - \frac{a_1}{a_2}P_1^{(3)}, \tag{25c}$$

where
$$\begin{aligned}
\xi_1 &= (\gamma_1-\gamma_2)\tilde{P_{1R}}\tilde{P_{2R}}P_2^{max} - \gamma_2(\gamma_1+1)\Delta\tilde{P_{1R}},\\
\zeta_1 &= -\gamma_2\tilde{P_{1R}}^2,\\
\varrho_1 &= \gamma_1\tilde{P_{2R}}^2 P_2^{max^2} + \gamma_1(\gamma_2+1)\Delta\tilde{P_{2R}}P_2^{max},\\
\xi_2 &= (\gamma_1-\gamma_2)\tilde{P_{1R}}\tilde{P_{2R}}P_1^{max} + \gamma_1(\gamma_2+1)\Delta\tilde{P_{2R}},\\
\zeta_2 &= \gamma_1\tilde{P_{2R}}^2,\\
\varrho_2 &= -\gamma_2\tilde{P_{1R}}^2 P_1^{max^2} - \gamma_2(\gamma_1+1)\Delta\tilde{P_{1R}}P_1^{max},\\
\xi_3 &= -\frac{2I_{th}a_1\gamma_1\tilde{P_{2R}}^2}{a_2^2} + \frac{(\gamma_1-\gamma_2)\tilde{P_{1R}}I_{th}}{a_2} - \frac{\gamma_1(\gamma_2+1)\Delta\tilde{P_{2R}}a_1}{a_2} - \gamma_2(\gamma_1+1)\Delta\tilde{P_{1R}},\\
\zeta_3 &= \frac{\gamma_1\tilde{P_{2R}}^2 a_1^2}{a_2^2} - \gamma_2\tilde{P_{1R}}^2 - \frac{(\gamma_1-\gamma_2)\tilde{P_{1R}}\tilde{P_{2R}}a_1}{a_2},\\
\varrho_3 &= \frac{\gamma_1\tilde{P_{2R}}^2 I_{th}^2}{a_2^2} + \frac{\gamma_1(\gamma_2+1)\Delta\tilde{P_{2R}}I_{th}}{a_2}.
\end{aligned}$$

TABLE I
COMPARISON OF RUNNING TIMES

Algorithms	Running Times
JTBPA	$\mathcal{O}(\log_2(\frac{t_{\text{up}}-t_{\text{low}}}{\eta})(M_1^{4.5}+M_2^{4.5}))$
MRT with Optimal Power	$\mathcal{O}(M_1^2+M_2^2)$
ZFB-MRT with Optimal Power	$\mathcal{O}(M_1^2+M_2^2)$

the conventional two-way relay network (SU_1, SU_2 and R) without any primary nodes and interference constraints. In this case, MRC is the optimal RX beamforming strategy for SU_j ($j=1,2$) to receive in the second time slot because it maximizes the received signal power at SU_j. In terms of Tx beamforming, MRT is selected to maximize the signal power for $SU_j \rightarrow$R ($j=1,2$) in the first time slot. Meanwhile, the maximum available power is selected at both SU_j ($j=1,2$) and R. The average achievable SINR over 10^3 simulation runs is chosen as the performance metric.

All the plots are generated with $N_0 = 0$ dBm and $P_p = 3$ dBm. Each channel coefficient is $\mathcal{CN}(0,1)$ distributed. To observe the impact of the maximum transmit power, we assume $P_1^{max} = P_2^{max} = P^{max}$ and choose 3 dBm and 10 dBm, respectively.

A. Achievable SINR vs. Interference Threshold I_{th}

Figures 3 to 5 plot the average SINR as a function of I_{th}. Note that the proposed JTBPA provides over 10 dB SINR improvement over EPA. Thus beamforming and power allocation exploit not only the spatial diversity, but also the

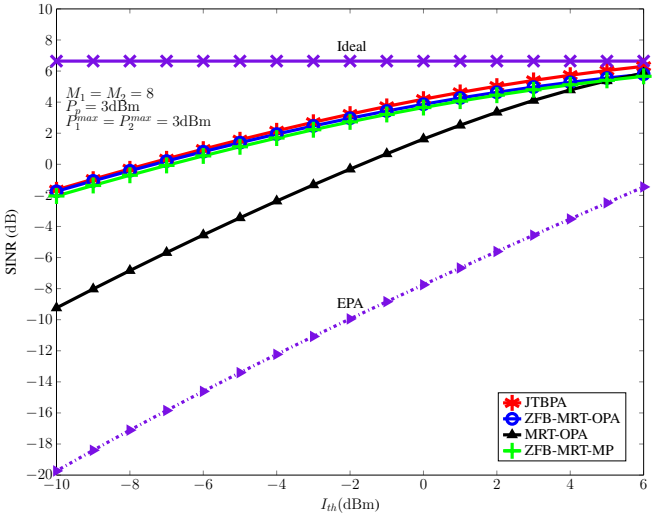

Fig. 3. SINR vs. I_{th} with $M_1 = M_2 = 8$ and $P_1^{mat} = P_2^{max} = 3$ dBm

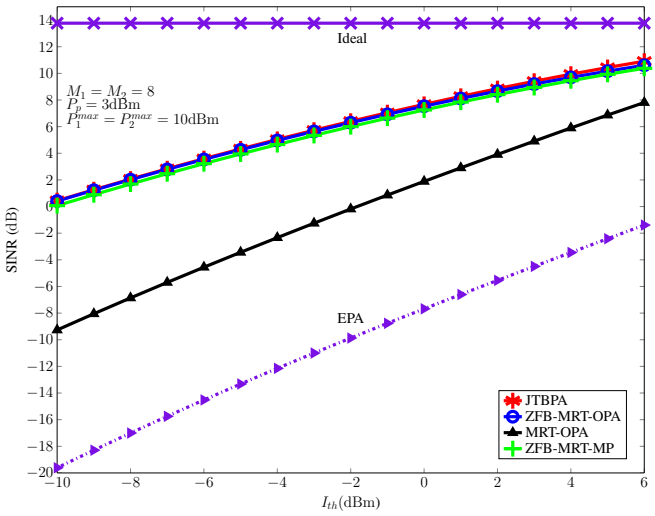

Fig. 4. SINR vs. I_{th} with $M_1 = M_2 = 8$ and $P_1^{mat} = P_2^{max} = 10\,\text{dBm}$

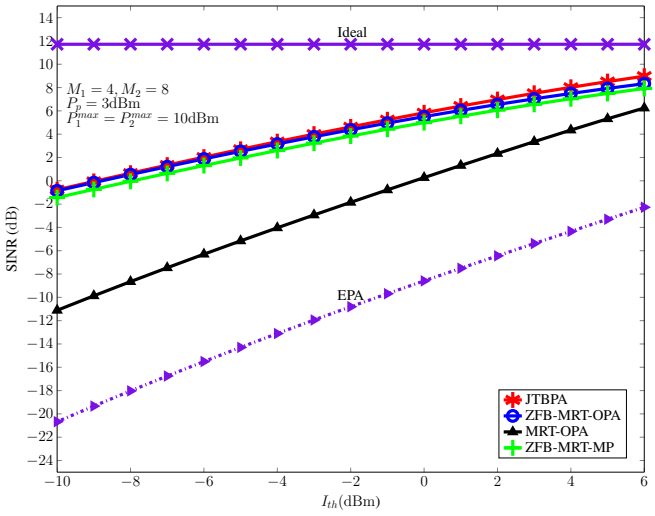

Fig. 5. SINR vs. I_{th} with $M_1 = 4$, $M_2 = 8$ and $P_1^{mat} = P_2^{max} = 10\,\text{dBm}$

interference threshold. Therefore, as expected, the gap between JTBPA and the Ideal case decreases with the increase in I_{th}, e.g. less than $4\,\text{dB}$ when $I_{th} = 6\,\text{dB}$ in Fig. 4. The reason for this SINR gap improvement is that at low interference thresholds, while beamforming at SU_j ($j = 1, 2$) partially eliminates $\text{SU}_j \rightarrow$PR interferences, the R$\rightarrow$PR interference dominates and hence relay transmit power must be low. But when PR has high interference tolerance, $I_{th} = 6\,\text{dB}$, the relay can transmit with higher power. Then cognitive beamforming exploits spatial diversities to improve the achievable SINR.

From Figs. 3 to 5, it is clear that ZFB-MRT-OPA can achieve almost the same performance as JTBPA in low interference temperature limit region (e.g. $I_{th} \leq 2\,\text{dBm}$ with the maximum transmit power of $10\,\text{dBm}$ and $I_{th} \leq -2\,\text{dBm}$ with maximum transmit power of $3\,\text{dBm}$). Figure 3 also shows that with the increase in the interference temperature limit (I_{th}), the gap between ZFB-MRT-OPA and JTBPA increases. This is because using ZFB-MRT, SU_j ($j = 1, 2$) causes no interference at PR. Therefore, the interference constraint is not exploited. The SINR loss due to not exploiting the interference constraint can be small when I_{th} is low, e.g. less than $0.5\,\text{dB}$ when $I_{th} = -10\,\text{dB}$ (Fig. 3). But when PR has high interference tolerance, e.g. $I_{th} = 6\,\text{dB}$, this SINR loss increases, e.g. $1\,\text{dB}$. However, this problem can be mitigated by either increasing the maximum transmit powers (Fig. 4) or equipping more antennas (Fig. 6).

With ZFB-MRT, optimal power allocation or maximum power transmission, a less than $1\,\text{dB}$ SINR gap exists throughout the entire interference temperature limit region ($[-10\,\text{dBm},\ 6\,\text{dBm}]$). This $1\,\text{dB}$ gap is because optimal power allocation provides a balance between terminals' and relay's transmissions. In other words, the relay node can transmit with a higher power than that when ZFB-MRT-MP is applied at the two terminals.

When comparing the performance of MRT-OPA in Figs. 3 and 4, we find that increasing the maximum transmit power does not benefit the achievable SINR, which is lower than the SINR obtained by JTBPA for over $5\,\text{dB}$ when $I_{th} \leq -4\,\text{dBm}$. But, as the interference temperature limit (I_{th}) increases, MRT-OPA converges to JTBPA. This convergence is reasonable because MRT aims at maximizing the desired signal power, which does not consider the interference factor. Consequently, to satisfy the interference constraint in low I_{th} region, the transmit power can not be high, regardless of the maximum available transmit power.

B. Achievable SINR vs. Number of Antennas M

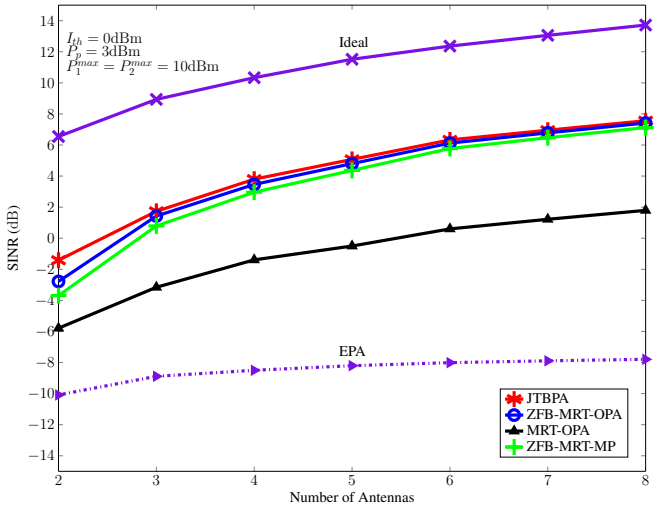

Fig. 6. SINR vs. Number of Antennas with $I_{th} = 0\,\text{dBm}$ and $P_1^{mat} = P_2^{max} = 10\,\text{dBm}$

Figure 6 shows the average SINR as a function of the number of antennas, where $M_1 = M_2$. Obviously increasing the number of antennas results in higher SINR due to the increasing spatial degrees of freedom. Thus the SINR gap between JTBPA and the ideal case is reduced from around $8\,\text{dB}$ to $6\,\text{dB}$. Thus, the capability of cognitive beamforming

in suppressing interference from/to the primary network is evident. As well, with the increase in the number of antennas, the SINR gap between ZFB-MRT-OPA/ZFB-MRT-MP and JTBPA has been reduced from over 2 dB with 2 antennas to less than 1 dB with 8 antennas. This is because, although ZFB-MRT does not exploit the interference threshold, the SINR loss of non-optimal beamforming coefficients can be partially overcome by exploiting more path diversities with more antennas. As mentioned before, with I_{th} =0 dBm, the transmit power determined by MRT-OPA is still relatively low because MRT has no control on the SU_j-to-PR ($j = 1, , 2$) interference. Therefore, a large SINR gap, e.g.over 5 dB, exists between MRT-OPA and JTBPA even when more antennas are equipped and more spatial diversities are exploited in MRT. Finally, it is obvious that since EPA has no beamforming, its achievable SINR remains relatively low, e.g. less than -8 dB, regardless of the increase in the number of antennas. Consequently, the gap between EPA and the ideal case is more than 16 dB.

C. Running Times Comparison

Table II shows the comparison of the total running time of 100 simulation runs in a computer equipped with Intel(R)i7-3770CPU at 3.4GHz using JTBPA, ZFB-MRT-OPA and MRT-OPA. In this comparison, I_{th}, P_j^{max} ($j = 1, 2$) are set to 0 dBm and 10 dBm, respectively. Clearly, the time complexity of JTBPA increases with the increasing number of antennas, while the timing of the other two methods is relatively constant.

VI. Conclusion

Cognitive beamforming for two underlay terminals (SU_1 and SU_2) and an underlay two-way AF relay (R) has been investigated in this paper. Beamforming was designed to maximize the worse SINR at SU_1 and SU_2. The optimal Rx beamforming vectors, which are computed directly from the CSIs, and which are independent from the transmit powers and the Tx beamforming vectors, and the optimal relay gain were derived. We also proposed a bi-section search based joint optimal algorithm (JTBPA) for the optimal Tx beamforming vectors and power allocations, and at each iteration SDR was used. Due to the relatively high computational complexity of JTBPA, we investigated MRT or ZFB-MRT for sub-optimal Tx beamforming, but the transmit power levels were optimally calculated. Numerical results show that JTBPA improves the achievable SINR by as much as 20 dB and comes within a few dBs from the performance of the ideal interference-free system. Besides, ZFB-MRT-OPA can achieve near optimal performance, e.g. SINR gap is less than 1 dB from JTBPA. Moreover, a fixed 1 dB SINR gap exists between the ZFB-MRT scheme with maximum transmit power and with optimal transmit power. On the other hand, MRT-OPA has a large performance gap (over 5 dB) from JTBPA in the low interference temperature region, e.g. $I_{th} \leq 0$ dBm. Overall, the main takeaway message from this work is that the interference issue in underlay network can be successfully mitigated. Thus spectral efficiency of the underlay concept can be realized. This work may be extended in several directions. First, optimal joint beamforming and power allocation can be developed for multi-antenna underlay devices, where multiple antennas at the relay node may be used to suppress both primary-to-relay and relay-to-primary interference signals. Second, optimal beamforming and power allocation can be developed considering CSI estimation errors, which arise in real applications.

References

[1] M. Ghosh. (2014, Jun.) 22 interesting insights on global mobile usage: Ericsson. [Online]. Available: http://trak.in/tags/business/2014/06/04/22-interesting-insights-global-mobile-usage/

[2] (2014, Feb.) Cisco visual networking index: Global mobile data traffic forecast update, 20132018. [Online]. Available: http://www.cisco.com/en/US/solutions/collateral/ns341/ns525/ns537/ns705/ns827/white_paper_c11-520862.html

[3] FCC, "FCC: In the matter of unlicensed operation in the TV broadcast bands docket 04-186 incremental reform ttoward a broadcast underlay, and the radio traffic signal," FCC2008, Tech. Rep., 2008.

[4] S. Haykin, "Cognitive radio: brain-empowered wireless communications," *IEEE J. Sel. Areas Commun.*, vol. 23, no. 2, pp. 201 – 220, Feb. 2005.

[5] W. Ajib and D. Haccoun, "An overview of scheduling algorithms in MIMO-based fourth-generation wireless systems," *IEEE Network*, vol. 19, no. 5, pp. 43–48, Sep. 2005.

[6] G. Boudreau, J. Panicker, N. Guo, R. Chang, N. Wang, and S. Vrzic, "Interference coordination and cancellation for 4G networks," *IEEE Commun. Mag.*, vol. 47, no. 4, pp. 74–81, Apr. 2009.

[7] S. Mohammad Razavizadeh, M. Ahn, and I. Lee, "Three-dimensional beamforming: A new enabling technology for 5G wireless networks," *IEEE Signal Process. Mag.*, vol. 31, no. 6, pp. 94–101, Nov. 2014.

[8] K. Ratajczak, K. Bakowski, and K. Wesolowski, "Two-way relaying for 5G systems: Comparison of network coding and MIMO techniques," in *2014 IEEE Wireless Commun. Networking Conf. (WCNC)*, Apr. 2014, pp. 376–381.

[9] W. Xu, J. Zhang, P. Zhang, and C. Tellambura, "Outage probability of decode-and-forward cognitive relay in presence of primary user's interference," *IEEE Commun. Lett*, vol. 16, no. 8, pp. 1252–1255, Aug. 2012.

[10] M. Chraiti, H. Hakim, W. Ajib, and H. Boujemaa, "Spectrum sharing techniques for broadcast cognitive radio networks," *IEEE Trans. Wireless Commun.*, vol. 12, no. 11, pp. 5880–5888, Nov. 2013.

[11] K. Cumanan, R. Krishna, L. Musavian, and S. Lambotharan, "Joint beamforming and user maximization techniques for cognitive radio networks based on branch and bound method," *IEEE Trans. Wireless Commun.*, vol. 9, no. 10, pp. 3082–3092, Oct. 2010.

[12] K. Cumanan, L. Musavian, S. Lambotharan, and A. Gershman, "SINR balancing technique for downlink beamforming in cognitive radio networks," *IEEE Signal Process. Lett.*, vol. 17, no. 2, pp. 133–136, Feb. 2010.

[13] N. Jamal and P. Mitran, "Performance tradeoffs offered by beamforming in cognitive radio systems: An analytic approach," *IEEE Trans. Wireless Commun.*, vol. 11, no. 10, pp. 3766–3777, Oct. 2012.

[14] M.-L. Ku, L.-C. Wang, and Y.-T. Su, "Toward optimal multiuser antenna beamforming for hierarchical cognitive radio systems," *IEEE Trans. Commun.*, vol. 60, no. 10, pp. 2872–2885, Oct. 2012.

[15] K. Phan, S. Vorobyov, N. Sidiropoulos, and C. Tellambura, "Spectrum sharing in wireless networks via QoS-aware secondary multicast beamforming," *IEEE Trans. Signal Process.*, vol. 57, no. 6, pp. 2323–2335, Jun. 2009.

[16] Y. Rahulamathavan, K. Cumanan, and S. Lambotharan, "A mixed SINR-balancing and SINR-target-constraints-based beamformer design technique for spectrum-sharing networks," *IEEE Trans. Veh. Technol.*, vol. 60, no. 9, pp. 4403–4414, Nov. 2011.

[17] R. Ramamonjison, A. Haghnegahdar, and V. Bhargava, "Joint optimization of clustering and cooperative beamforming in green cognitive wireless networks," *IEEE Trans. Wireless Commun.*, vol. 13, no. 2, pp. 982–997, Feb. 2014.

TABLE II
RUNNING TIMES

	JTBPA	ZFB-MRT-OPA	MRT-OPA
$M_1 = M_2 = 4$	73.463s	0.014s	0.018s
$M_1 = 4,\ M_2 = 8$	90.774s	0.010s	0.010s
$M_1 = M_2 = 8$	110.707s	0.010s	0.009s

[18] G. Huang and J. Tugnait, "On energy efficient MIMO-assisted spectrum sharing for cognitive radio networks," in *Proc. 2013 IEEE Int. Conf. Commun. (ICC)*, Jun. 2013, pp. 2644–2649.

[19] R. Zhang and Y.-C. Liang, "Exploiting multi-antennas for opportunistic spectrum sharing in cognitive radio networks," *IEEE J. Sel. Topics Signal Process.*, vol. 2, no. 1, pp. 88–102, Feb. 2008.

[20] R. Zhang, F. Gao, and Y.-C. Liang, "Cognitive beamforming made practical: Effective interference channel and learning-throughput tradeoff," *IEEE Trans. Commun.*, vol. 58, no. 2, pp. 706–718, Feb. 2010.

[21] S.-M. Cai and Y. Gong, "Cognitive beamforming for multiple secondary data streams with individual SNR constraints," *IEEE Trans. Signal Process.*, vol. 61, no. 17, pp. 4189–4198, Sep. 2013.

[22] A. Piltan, S. Salari, D. Mirzahosseini, and M. Peyghami, "Filter-and-forward relay beamforming in cognitive two-way relay networks," in *2011 IEEE 5th Int. Conf. Advanced Networks and Telecommun. Systems (ANTS)*, Dec. 2011, pp. 1–5.

[23] X. Zhang, Z. Zhang, J. Xing, R. Yu, P. Zhang, and W. Wang, "Exact outage analysis in cognitive two-way relay networks with opportunistic relay selection under primary user's interference," *IEEE Trans. Veh. Technol.*, vol. 64, no. 6, pp. 2502–2511, Jun. 2015.

[24] T. Luan, F. Gao, X.-D. Zhang, J. Li, and M. Lei, "Rate maximization and beamforming design for relay-aided multiuser cognitive networks," *IEEE Trans. Veh. Technol.*, vol. 61, no. 4, pp. 1940–1945, May 2012.

[25] M. Beigi and S. Razavizadeh, "Cooperative beamforming in cognitive radio networks," in *2009 2nd IFIP Wireless Days (WD)*, Dec. 2009, pp. 1–5.

[26] A. Piltan, S. Salari, and R. Sadeghzadeh, "Network beamforming in cognitive relay networks with QoS constraints," in *2011 IFIP Wireless Days (WD)*, Oct. 2011, pp. 1–3.

[27] A. Piltan and S. Salari, "Distributed beamforming in cognitive relay networks with partial channel state information," *IET Commun.*, vol. 6, no. 9, pp. 1011–1018, Jun. 2012.

[28] K. Zarifi, S. Affes, and A. Ghrayeb, "Joint power control and relay design in underlay cognitive networks with multiple transmitter-receiver pairs," in *Proc. 2011 Conf. Record Forty Fifth Asilomar Conf. Signals, Systems and Computers (ASILOMAR)*, Nov. 2011, pp. 1216–1221.

[29] S. Safavi, M. Ardebilipour, and S. Salari, "Relay beamforming in cognitive two-way networks with imperfect channel state information," *IEEE Wireless Commun. Lett.*, vol. 1, no. 4, pp. 344–347, Aug. 2012.

[30] Y. CAO and C. Tellambura, "Joint distributed beamforming and power allocation in underlay cognitive two-way relay links using second-order channel statistics," *IEEE Trans. Signal Process.*, vol. 62, pp. 5950–5961, Nov. 2014.

[31] T. M. Chinh Chu, H. Phan, T. Q. Duong, M. Elkashlan, and H.-J. Zepernick, "Beamforming transmission in cognitive AF relay networks with feedback delay," in *Proc. Int. Conf. in Comput., Manage. and Telecommun. (ComManTel)*, Jan. 2013, pp. 117–122.

[32] Y. Cao and C. Tellambura, "Outage analysis of ZFB-MRT/MRC underlay two-way relay systems," *IEEE Commun. Lett*, vol. 19, no. 6, pp. 1049–1052, Jun. 2015.

[33] N. Yang, P. Yeoh, M. Elkashlan, I. Collings, and Z. Chen, "Two-way relaying with multi-antenna sources: Beamforming and antenna selection," *IEEE Trans. Veh. Technol.*, vol. 61, no. 9, pp. 3996–4008, Nov. 2012.

[34] D. Tse, P. Viswanath, and L. Zheng, "Diversity-multiplexing tradeoff in multiple-access channels," *Information Theory, IEEE Transactions on*, vol. 50, no. 9, pp. 1859–1874, Sept 2004.

[35] Z.-Q. Luo, W.-K. Ma, A.-C. So, Y. Ye, and S. Zhang, "Semidefinite relaxation of quadratic optimization problems," *IEEE Signal Processing Mag.*, vol. 27, no. 3, pp. 20–34, May 2010.

[36] T. M. C. Chu, T. Duong, and H. Zepernick, "Performance analysis for multiple-input multiple-output-maximum ratio transmission systems with channel estimation error, feedback delay and co-channel interference," *IET Commun.*, vol. 7, no. 4, pp. 279–285, Mar. 2013.

[37] L. Zhao, K. Zheng, H. Long, H. Zhao, and W. Wang, "Performance analysis for downlink massive multiple-input multiple-output system with channel state information delay under maximum ratio transmission precoding," *IET Commun.*, vol. 8, no. 3, pp. 390–398, Feb. 2014.

[38] Y. Chen and C. Tellambura, "Performance analysis of maximum ratio transmission with imperfect channel estimation," *IEEE Commun. Lett.*, vol. 9, no. 4, pp. 322–324, Apr. 2005.

[39] J. G. Proakis and M. Salehi, *Digital Communications*, 5th ed. McGraw-Hill Science/Engineering/Math, Nov. 2007.

[40] T. K. Y. Lo, "Maximum ratio transmission," *IEEE Trans. Commun.*, vol. 47, no. 10, pp. 1458–1461, Oct. 1999.

[41] A. Afana, V. Asghari, A. Ghrayeb, and S. Affes, "On the performance of cooperative relaying spectrum-sharing systems with collaborative distributed beamforming," *IEEE Trans. Commun.*, vol. 62, no. 3, pp. 857–871, Mar. 2014.

[42] S. Song, M. Hasna, and K. Letaief, "Prior zero forcing for cognitive relaying," *IEEE Trans. Wireless Commun.*, vol. 12, no. 2, pp. 938–947, Feb. 2013.

[43] H. Katiyar and R. Bhattacharjee, "Performance of regenerative relay network operating in uplink of multi-antenna base station under Rayleigh fading channel," in *Proc. TENCON 2009 - 2009 IEEE Region 10 Conf.*, Jan. 2009, pp. 1–5.

[44] D. Senaratne and C. Tellambura, "Beamforming for space division duplexing," in *2011 IEEE Int. Conf. Commun. (ICC)*, Jun. 2011, pp. 1–5.

[45] M. Zeng, R. Zhang, and S. Cui, "On design of collaborative beamforming for two-way relay networks," *IEEE Trans. Signal Process.*, vol. 59, no. 5, pp. 2284–2295, May 2011.

[46] J. Lee, H. Wang, J. Andrews, and D. Hong, "Outage probability of cognitive relay networks with interference constraints," *IEEE Trans. Wireless Commun.*, vol. 10, no. 2, pp. 390–395, Feb. 2011.

[47] T. Cui, C. Tellambura, and Y. Wu, "Low-complexity pilot-aided channel estimation for OFDM systems over doubly-selective channels," in *Proc. 2005 IEEE Int. Conf. Commun.*, vol. 3. IEEE, May 2005, pp. 1980–1984.

[48] Z. Zhang, W. Zhang, and C. Tellambura, "Cooperative OFDM channel estimation in the presence of frequency offsets," *IEEE Trans. Veh. Technol.*, vol. 58, no. 7, pp. 3447–3459, Sep. 2009.

[49] G. Wang and C. Tellambura, "Super-imposed pilot-aided channel estimation and power allocation for relay systems," in *2009 IEEE Wireless Commun. and Networking Conf. (WCNC)*, Apr. 2009, pp. 1–6.

[50] G. Wang, F. Gao, and C. Tellambura, "Superimposed pilot based joint CFO and channel estimation for CP-OFDM modulated two-way relay networks," in *2010 IEEE Global Telecommun. Conf.*, Dec. 2010, pp. 1–5.

[51] Z. Dai, J. Liu, C. Wang, and K. Long, "An adaptive cooperation communication strategy for enhanced opportunistic spectrum access in cognitive radios," *IEEE Commun. Lett.*, vol. 16, no. 1, pp. 40–43, Jan. 2012.

[52] A. Afana, A. Ghrayeb, V. Asghari, and S. Affes, "Distributed beamforming for spectrum-sharing systems with AF cooperative two-way relaying," *IEEE Trans. Commun.*, vol. 62, no. 9, pp. 3180–3195, Sep. 2014.

[53] S. Puntanen, G. P. Styan, and J. Isotalo, *Matrix Tricks for Linear Statistical Models: our personal top twenty*. Springer, 2011.

[54] W. H. Press, S. A. Teukolsky, W. T. Vetterling, and B. P. Flannery, "Numerical recipes in C: The art of scientific computing. second edition," 1992.

[55] S. Boyd and L. Vandenberghe, *Convex Optimization*. Cambridge, U.K.: Cambridge Univ. Press, 2004.

[56] Y. Huang and S. Zhang, "Complex matrix decomposition and quadratic programming," *Math. Oper. Res.*, vol. 32, pp. 758–768, Aug. 2007.
[57] T. H. Cormen, C. E. Leiserson, R. L. Rivest, and C. Stein, *Introduction to algorithms*. The MIT Press, 2009.

Yun CAO received the B.Sc. degree in automation from Southeast University, China in 2007, the M.Eng. degree in automation from Southeast University, China in 2010, and the Ph.D. degree in electrical and computer engineering at the University of Alberta, Edmonton, Alberta, Canada in 2015. Her research interests include beamforming and power allocation in cooperative cognitive relay networks, and performance analysis in cognitive networks.

Chintha Tellambura (F'11) received the B.Sc. degree (with first-class honor) from the University of Moratuwa, Sri Lanka, in 1986, the M.Sc. degree in Electronics from the University of London, U.K., in 1988, and the Ph.D. degree in Electrical Engineering from the University of Victoria, Canada, in 1993.
He was a Postdoctoral Research Fellow with the University of Victoria (1993-1994) and the University of Bradford (1995-1996). He was with Monash University, Australia, from 1997 to 2002. Presently, he is a Professor with the Department of Electrical and Computer Engineering, University of Alberta. His research interests focus on communication theory dealing with the wireless physical layer.
Prof. Tellambura is an Associated Editor for the IEEE TRANSACTIONS ON COMMUNICATION and the Area Editor for Wireless Communications Systems and Theory in the IEEE TRANSACTIONS ON WIRELESS COMMUNICATIONS. He was Chair of the Communication Theory Symposium in Globecom'05 held in St. Louis, MO.